Chen's lattice inversion embedded-atom method for Ni–Al alloy*

Zhang Chuan-Hui(张川晖)†, Huang Shuo(黄 烁), Shen Jiang(申 江), and Chen Nan-Xian(陈难先)

University of Science and Technology Beijing, Institute of Applied Physics, Beijing 100083, *China*

(Received 21 May 2012; revised manuscript received 3 July 2012)

The structural properties, the enthalpies of formation, and the mechanical properties of some Ni–Al intermetallic compounds (NiAl, Ni_3Al, $NiAl_3$, Ni_5Al_3, Ni_3Al_4) are studied by using Chen's lattice inversion embedded-atom method (CLI-EAM). Our calculated lattice parameters and cohesive energies of Ni–Al compounds are consistent with the experimental and the other EAM results. The results of enthalpy of formation indicate a strong chemical interaction between Ni and Al in the intermetallic compounds. Through analyzing the alloy elastic constants, we find that all the Ni–Al intermetallic compounds discussed are mechanically stable. The bulk moduli of the compounds increase with the increasing Ni concentration. Our results also suggest that NiAl, Ni_3Al, $NiAl_3$, and Ni_5Al_3 are ductile materials with lower ratios of shear modulus to bulk modulus; while Ni_3Al_4 is brittle with a higher ratio.

Keywords: embedded-atom method, lattice inversion, NiAl alloy, mechanical property

PACS: 34.20.–b, 61.66.Dk, 62.20.–x **DOI:** 10.1088/1674-1056/21/11/113401

1. Introduction

The Ni–Al intermetallic compound has attracted much attention in recent years for its high melting temperature, good oxidation resistance, high thermal conductivity, and low density.[1–4] Many researchers have studied the B_2 type NiAl and the $L1_2$ type Ni_3Al compounds, e.g., the mechanical properties of NiAl could be improved by alloying with ternary additions,[5–7] and the types of point defects in Ni_3Al were discussed, and it was shown that the point defect is the antisite defect in the nonstoichiometric case.[8] However, the other Ni–Al intermetallic compounds are less studied.

In 2011, Wang *et al.* predicted the enthalpies of formation and the elastic constants by using the density functional theory (DFT), which provides a helpful insight into the properties of the Ni–Al intermetallic compounds.[2] Then Xiang *et al.* showed that the Ni_5Al_3 phase layer starts to form only when the outer layer is completely consumed and that the growth kinetics of each of the intermediate layers differs from that of its subsequent consumption.[9] And the replacement of Ni by 10 at.% Co in the $Ni_{66}Al_{34}$ alloy decreased the tendency to the formation of the Ni_5Al_3 phase.[10] In 2008, the $NiAl_3$ intermetallic compound with particle size less than 100 nm was prepared by a novel patented solid-liquid reaction milling technology.[11] Li *et al.* studied two critical compositions, which had 7.9% and 13.1% $NiAl_3$ in Al–15%Mg_2Si–$NiAl_3$ system, differences in the formation of $NiAl_3$ intermetallic particles and the microstructure during the solidification interval were found.[12] Using an excimer KrF, the ablation of the Ni_3Al target led to the matrix comprising the nanocrystalline Ni_3Al_4 cubic phases.[13]

Since 1990, Chen's lattice inversion[14] has been widely applied to obtain the pair potentials from the first-principles calculations. For example, Zhang *et al.*[15] firstly obtained the pair interaction in the Finnis–Sinclair[16] and the embedded-atom method (EAM) potentials using Chen's inversion formula. And the inversion method has been applied to ionic crystals,[17] metal-ceramic interfaces,[18] rare earth transition intermetallic compounds,[19] semiconductors,[20] and actinicles intermetallics.[21,22] It is noteworthy that the interatomic pair potential can be strictly acquired to arbitrary-distance neighbor by using Chen's lattice inversion.

In this paper, we construct a new alloy potential based on a pure metal Chen's lattice inversion embedded-atom method (CLI-EAM).[23] Then we apply the method to Ni–Al intermetallic compounds (NiAl, Ni_3Al, $NiAl_3$, Ni_5Al_3, Ni_3Al_4) to investigate their stabilities of structure and mechanical proper-

*Project supported by the National Basic Research Program of China (Grant No. 2011CB606401).

†Corresponding author. E-mail: ym23_24@yahoo.com.cn

© 2012 Chinese Physical Society and IOP Publishing Ltd

ties.

2. Method of calculation

In the present paper, we use the CLI-EAM to calculate all the results. This method was proposed by the authors based on the first principles, and has simulated fcc metals Au, Ag, Cu, and Pt successfully.[23] For the binary alloy EAM, the cohesive energy $E_{\rm tot}$ is written as

$$E_{\rm tot} = E_1 + E_2 + \Delta E, \tag{1}$$

$$E_1 = F_1(\rho_1) + \frac{1}{2}\sum \Phi_{11}, \tag{2}$$

$$E_2 = F_2(\rho_2) + \frac{1}{2}\sum \Phi_{22}, \tag{3}$$

where E_1, E_2, and ΔE are the cohesive energy of metal A, the cohesive energy of metal B, and the residual cohesive energy, respectively, and Φ_{11} and Φ_{22} are the interatomic pair potentials of metals A and B, respectively. In general, the cohesive energy per atom of the crystal can be express as the sum of interatomic pair potentials, so we get

$$\Delta E = \sum_n r(n)\Phi_{12}\left[b(n)r_{1\rm e}\right], \tag{4}$$

where Φ_{12} is the pair potential between atoms 1 and 2, $r_{1\rm e}$ is the distance to the nearest neighbor, $r(n)$ is the number of n-th neighbor atoms, and $b(n)$ is the ratio of the n-th neighbor distance to the first neighbor distance. Based on Chen's lattice inversion,[14] the pair potential between different atoms is assumed to be

$$\Phi_{12} = \sum_n I(n)\Delta E\left[b(n)r_{1\rm e}\right], \tag{5}$$

where $I(n)$ is the inversion coefficient depending only on the structure (we use the inversion coefficient of the B2 structure in this paper), and can be written as

$$\sum_{b(n)|b(m)} I(n)r\left(b^{-1}\left[\frac{b(m)}{b(n)}\right]\right) = \delta_{m1}. \tag{6}$$

The form of pair potential function is proposed to use the Morse function[24]

$$\Phi(r) = D_0(\exp[-2\alpha_0(r-r_0)] - 2\exp[-\alpha_0(r-r_0)]). \tag{7}$$

The basic equations of the embedded atom method are[25,26]

$$E(r) = F(\rho) + \frac{1}{2}\sum \Phi(r), \tag{8}$$

$$\rho(r) = \sum f(r), \tag{9}$$

where $E(r)$ is the cohesive energy of each atom in metal, $F(\rho)$ is the energy to embed one atom in the background electron density, ρ is the background electron density (BED) at one atom due to all other atoms, and $\Phi(r)$ is the repulsive pair potential between different atoms. Thus, ρ is assumed to be a linear combination of contributions from $f(r)$, here $f(r)$ is the atomic electron density (AED) and is a function of distance from the center, r is the distance between different atoms.

The form of embedding energy F is proposed by Banerjea and Smith,[27] they put forward another form of embedding function based on the effective medium theory[28] and the universal energy function given by Rose.[29] The functions of BED and AED each have an exponentially decreasing form

$$F(\rho) = -F_0\left[1 - n\ln(\rho/\rho_0)\right](\rho/\rho_0)^n, \tag{10}$$

$$\rho(r) = \rho_{\rm e}\exp\left[-\lambda(r/r_{1\rm e}-1)\right], \tag{11}$$

$$f(r) = f_{\rm e}\exp\left[-\beta(r/r_{1\rm e}-1)\right]. \tag{12}$$

All the input parameters for calculations are listed in Table 1.

Table 1. The input parameters for background electron density, atomic electron density, embedding function, pair potential of Ni and Al, and the pair potential between different atoms in the Ni–Al alloy.

	$\rho(r)$		$f(r)$		$F(\rho)$		$\Phi(r)$		
	$\rho_{\rm e}/$Å^{-3}	λ	$f_{\rm e}/$Å^{-3}	β	n	F_0	D_0	α_0	R_0
Al	0.0194	7.275	0.00159	6.951	0.364	1.075	0.214	1.322	2.836
Ni	0.0325	6.355	0.00249	6.181	0.672	2.584	0.220	1.713	2.648
Ni–Al							0.586	1.684	2.721

The moduli are obtained by using Voigt, Reuss, and Hill (VRH) approximations.[30] The bulk modulus B and the shear modulus G are obtained from the elastic constants

$$B = \frac{1}{9}\left[C_{11} + C_{22} + C_{33} + 2\left(C_{12} + C_{13} + C_{23}\right)\right], \tag{13}$$

$$G = \frac{1}{15}[C_{11} + C_{22} + C_{33} + 2\,(C_{44} + C_{55} + C_{66}) - C_{12} - C_{13} - C_{23}]. \quad (14)$$

The Young's modulus Y and the Poisson's modulus ν are obtained from the bulk modulus B and the shear modulus G

$$Y = \frac{9BG}{3B + G}, \quad (15)$$

$$\nu = \frac{3B - 2G}{2(3B + G)}. \quad (16)$$

3. Results and discussion

3.1. Structural properties

Based on phase diagrams, there are some Ni–Al intermetallic compounds confirmed in experiments, namely, $NiAl_3$, Ni_3Al_4, NiAl, Ni_5Al_3, and Ni_3Al. Whereas there are few available EAM potentials for all these intermetallic compounds, so the CLI-EAM Ni–Al alloy potential is used to calculate the lattice parameters, the enthalpies of formation, and the cohesive energies of these compounds. The results are shown in Table 2. We can see that some EAM potentials can well describe the structural and the energetic properties of the compounds.[8,31–35] In the CLI-EAM method, the Morse function[24] is used to describe the energy of crystal, so the acquired lattice constant and cohesive energy of the NiAl compound are consistent with the experimental[36,37] and the other EAM results.[8,31–35] Then we apply this alloy potential to five other Ni–Al intermetallic compounds. Our calculated lattice parameters of all the compounds are consistent with the relevant experimental results except $NiAl_3$ ($a = 6.966$ Å, $b = 7.761$ Å, $c = 5.070$ Å) with a difference of 5.6%. At the same time, our calculated cohesive energies of all the compounds are consistent with the relevant experimental results except Ni_5Al_3 ($E_c = 4.743$ eV) with a difference of 4.7%. These differences may be attributed to the center-symmetry model of the CLI-EAM, which does not describe the non-close-packed crystal (such as orthorhombic structure $NiAl_3$ and Ni_5Al_3) well. Although our results are not as consistent with the experimental ones as some EAM calculations, our potential can well describe the structures and the energies of all the compounds with acceptable differences. As we know, the portability of potential is a very important character in atomic scale simulation, therefore, the CLI-EAM potential has good portability for Ni–Al intermetallic compounds.

Table 2. The calculated lattice parameters, enthalpies of formation, and cohesive energies of Ni–Al intermetallic compounds.

	Method	Lattice parameter/Å	E_c/eV	H_f/kJ·mol^{-1}
NiAl	CLI-EAM	2.894	–4.514	–59.0
	MAEAM[31]	a=2.964	–4.326	–39.6
	EAM[32]	a=2.86	–4.470	
	EAM[33]	a=2.88	–4.49	
	GEAM[34]	a=2.973	–3.95	
	EAM[35]	a=2.906	–4.316	
	exp.	a=2.887[36], a=2.88[40]	–4.525[37], –4.50[37]	–67.7[38], –65.7[39]
Ni_3Al	CLI-EAM	a=3.531	–4.550	–35.8
	MAEAM[31]	a=3.563	–4.662	–46.4
	EAM[32]	a=3.525	–4.600	
	EAM[8]	a=3.566	–4.632	
	EAM[33]	a=3.56	–4.66	
	GEAM[34]	a=3.607	–4.20	
	EAM[35]	a=3.566	–4.632	
	exp.	a=3.566[36]	–4.557[37], –4.57[37]	–47.4[38], –39.6[39]
$NiAl_3$	CLI-EAM	a=6.966, b=7.761, c=5.070	–4.141	–47.4
	EAM[32]	a=6.415, b=7.484, c=4.950	–3.914	
	exp.	a=6.598[36], b=7.352[36], c=4.802[36]	–4.02[41]	–37.7[37]
Ni_3Al_4	CLI-EAM	a=11.353	–4.012	-58.0
	EAM[32]	a=11.375	–4.283	
	exp.	a=11.408[36]		
Ni_5Al_3	CLI-EAM	a=7.425, b=6.667, c=3.390	–4.743	–67.7
	EAM[42]	a=7.5, b=6.6, c=3.75	–4.596	
	exp.	a=7.44[36], b=6.68[36], c=3.72[36]	–4.53[33]	

Through studying the energies of optimized Ni–Al intermetallic compounds and fcc metals Ni and Al, we can obtain the enthalpies of formation (H_f) for Ni–Al compounds. As shown in Table 2, our results are consistent with the available experimental[37–39] and EAM results.[31] The results are compared in Fig. 1, we find that the Ni_5Al_3 alloy has the largest H_f (67.7 kJ/mol). The absolute values of H_f for $NiAl_3$, Ni_3Al_4, NiAl, Ni_5Al_3, and Ni_3Al are 47.4 kJ/mol, 58.0 kJ/mol, 59.0 kJ/mol, 67.7 kJ/mol, and 35.8 kJ/mol, respectively, meaning there are very strong chemical interactions between Ni and Al atoms. Therefore all the Ni–Al intermetallic compounds are thermodynamically stable due to the negative enthalpies of formation.

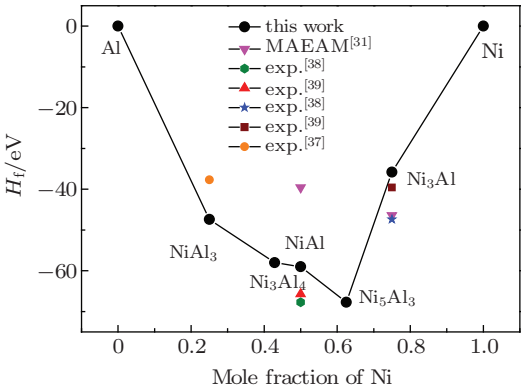


Fig. 1. (colour online) Calculated enthalpies of formation for Ni–Al intermetallic compounds.

3.2. Elastic properties and mechanical stability

In this section, we study the mechanical stability of the Ni–Al intermetallic compounds, the elastic constants are investigated by using the CLI-EAM alloy potential. All the results are shown in Table 3 together with the experimental[43–46] and the EAM calculation[31,32,34,35,42] results. Our calculated elastic constants of NiAl and Ni_3Al are consistent with the experimental and the EAM theoretical data, while smaller differences exist for Ni_3Al. The mechanical stability leads to restrictions on the elastic constants. For cubic structures (NiAl, Ni_3Al, and Ni_3Al_4),[47] we have

$$C_{11} > 0,\ C_{44} > 0,\ C_{11} - C_{12} > 0,\ C_{11} + 2C_{12} > 0. \quad (17)$$

And for orthorhombic structures ($NiAl_3$ and Ni_5Al_3),[48] we have

$$\begin{aligned} &C_{11} > 0, \quad C_{22} > 0, \quad C_{33} > 0, \\ &C_{44} > 0, \quad C_{55} > 0, \quad C_{66} > 0, \\ &C_{11} + C_{22} - 2C_{12} > 0, \quad C_{11} + C_{33} - 2C_{13} > 0, \\ &C_{22} + C_{33} - 2C_{23} > 0, \\ &C_{11} + C_{22} + C_{33} + 2\,(C_{12} + C_{13} + C_{23}) > 0. \end{aligned} \quad (18)$$

From Table 2, we find that all the elastic constants of the Ni–Al intermetallic compounds satisfy the above restrictions. Therefore all the Ni–Al compounds calculated by the CLI-EAM are mechanically stable.

Table 3. The calculated elastic properties (C_{ij} in units of GPa) of Ni–Al intermetallic compounds.

	Method	C_{11}	C_{12}	C_{13}	C_{22}	C_{23}	C_{33}	C_{44}	C_{55}	C_{66}
NiAl	CLI-EAM	195.5	139.0					107.3		
	EAM[32]	200	140					120		
	MAEAM[31]	188	132					100		
	EAM[42]	185.8	123.4					123.4		
	GEAM[8]	192.3	163.2					65.0		
	EAM[35]	182.6	115.8					92.6		
	exp.	199[43], 211[44]	137[43], 143[44]					116[43], 112[44]		
Ni_3Al	CLI-EAM	237.1	157.5					114.8		
	MAEAM[31]	192	127					97		
	EAM[38]	220.6	145.7					123.8		
	EAM[42]	214.7	113.8					113.8		
	GEAM[8]	260.8	156.7					64.2		
	EAM[35]	218.3	119.7					102.9		
	exp.	169[45], 225[46]	121[45], 149[46]					89[45], 124[46]		
Ni_3Al_4	CLI-EAM	273.4	54.9	54.9	231.5	109.4	231.5	59.2	31.9	31.9
$NiAl_3$	CLI-EAM	232.9	80.3	80.3	314.8	149.4	314.8	100.0	46.8	46.8
Ni_5Al_3	CLI-EAM	340.6	73.1	168.5	360.9	167.2	191.1	109.5	110.8	48.1

In order to better understand the mechanical properties of the Ni–Al intermetallic compounds, we calculate the bulk modulus B, the shear modulus G, the Young's modulus Y, and the Poisson's modulus ν and compare them with the experimental and the EAM results. As shown in Table 4, the calculated bulk modulus (184 GPa), shear modulus (61.8 GPa), and Young's modulus (166.7 GPa) of Ni_3Al are different from the experimental date of 174 GPa,[46] 77 GPa, and 202 GPa,[46] respectively. The differences may be attributed to two reasons. One is that the defects in the materials are not considered in our calculations; the other is that the effects of anisotropy on the elastic properties are not considered in experiments.

Table 4. The calculated bulk modulus B, shear modulus G, Young's modulus Y, and Poisson's modulus ν of Ni–Al intermetallic compounds.

	Method	B/GPa	G/GPa	Y/GPa	G/B	ν
NiAl	CLI-EAM	157.8	60.6	161.2	0.38	0.33
	EAM[42]	144.2				
	EAM[33]	144.2				
	exp.	156[52], 158[43]				
Ni_3Al	CLI-EAM	184.0	61.8	166.7	0.34	0.35
	exp.	174[46]	77[46]	210[53], 202[46]		
Ni_3Al_4	CLI-EAM	127.7	82.1	202.8	0.65	0.24
$NiAl_3$	CLI-EAM	164.7	62.6	166.7	0.38	0.33
Ni_5Al_3	CLI-EAM	180.1	68.0	181.2	0.38	0.33

To interpret our results, we show the bulk modulus, the shear modulus, and the Young's modulus for different Ni concentrations in Figs. 2 and 3. As can be seen, the calculated bulk moduli of NiAl and Ni_3Al are consistent with the experimental data, and the bulk moduli of the compounds increase with the increasing Ni concentration expect $NiAl_3$. The reason may be that a slightly larger total energy of the orthorhombic structure leads to a slightly larger elastic constant, and then the larger elastic constant leads to a larger bulk modulus. In Fig. 3, the Ni_3Al_4 alloy has the highest shear modulus and Young's modulus, whereas the NiAl alloy has the lowest values. Haines *et al.* proved that the hardness of a material is closely related to its shear modulus and Young's modulus.[49] Although the relationships between the hardness and the modulus are not universal, we believe that the larger the modulus is, the higher hardness the material has. Therefore, the Ni_3Al_4 alloy with the largest modulus (G = 82.1 GPa, Y = 202.8 GPa) is in the hard phase, while the NiAl alloy with the smallest modulus (G = 60.6 GPa, Y = 161.2 GPa) is in the soft phase. To study the brittleness and the ductility properties of the Ni–Al compounds, the ratio of shear modulus to bulk modulus (G/B), which is an empirical criterion of the extent of fracture range of the material,[50] is studied. According to Table 4, NiAl, Ni_3Al, $NiAl_3$, and Ni_5Al_3 are ductile materials, which have lower G/B values of 0.38, 0.34, 0.38, and 0.38, respectively; while Ni_3Al_4 is a brittle material with a higher G/B value of 0.65. Our results are consistent with the experimental results in Ref. [51], which showed that the fine grain NiAl alloy exhibits ductility because of the composition homogeneity by a rapid solidification processing. However, at room temperature, the bulk material of NiAl is brittle. This disagreement may be attributed to the center-symmetry model or the defects in the materials not considered in our calculations.

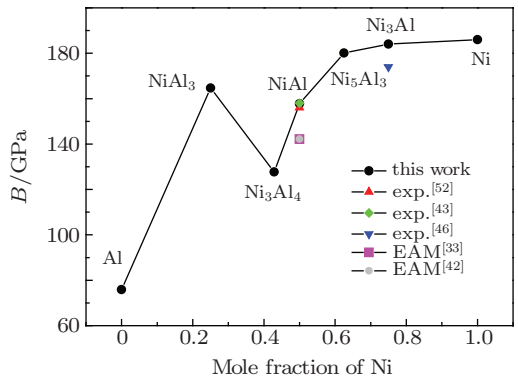


Fig. 2. (colour online) Calculated bulk moduli of Ni–Al intermetallic compounds.

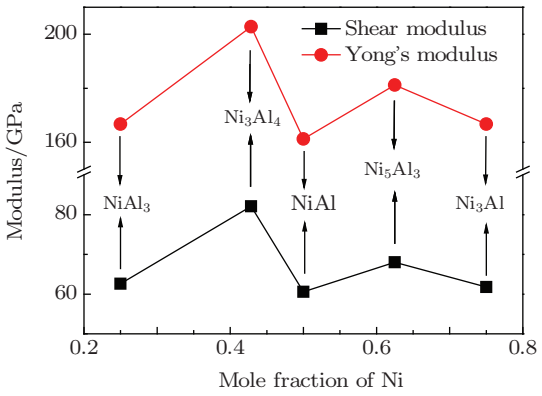


Fig. 3. (colour online) Calculated shear moduli and Young's moduli versus concentration of Ni for Ni–Al intermetallic compounds.

4. Conclusion

In this paper, we investigated the structural stability and the mechanical properties of Ni–Al intermetallic compounds (NiAl, Ni_3Al, $NiAl_3$, Ni_5Al_3, Ni_3Al_4) by using Chen's lattice inversion embedded-atom method. Our calculated lattice parameters and cohesive energies of the Ni–Al alloy are consistent with the experimental and the EAM results. There is a strong chemical interaction between Ni and Al in the intermetallic compounds because of the large enthalpies of formation. Through analyzing the crystal elastic constants, we find that all the Ni–Al intermetallic compounds discussed here are mechanically stable. The bulk moduli of the compounds increase with the increasing Ni concentration. The Ni_3Al_4 alloy with the largest bulk modulus and Young's modulus is in the hard phase, while the NiAl alloy with the smallest modulus is in the soft phase. The NiAl, Ni_3Al, $NiAl_3$, and Ni_5Al_3 are considered to be ductile materials, which have lower B/G values; while Ni_3Al_4 is considered to be a brittle material with a higher B/G value.

References

[1] Moverare J J, Johansson S and Reed R C 2009 *Acta Mater.* **57** 2266

[2] Wang J, Shang S L, Wang Y, Mei Z G, Liang Y F, Du Y and Liu Z K 2011 *Calphad* **35** 562

[3] Curtarolo S, Morgan D and Ceder G 2005 *Calphad* **29** 163

[4] Shi D M, Wen B, Melnik R, Yao S and Lia T J 2009 *J. Solid State Chem.* **182** 2664

[5] Zhang C L, Han P D, Li J M, Chi M, Yan L Y, Liu Y P, Liu X G and Xu B S 2008 *J. Phys.* D: *Appl. Phys.* **41** 095410

[6] Zhang Y X, Wang J C, Yang Y J, Yang G C and Zhou R H 2009 *Chin. Phys.* B **18** 4407

[7] Fan T Y and Li W 2011 *Chin. Phys.* B **20** 036101

[8] Yu S, Wang C Y and Yu T 2007 *Acta Phys. Sin.* **56** 3212 (in Chinese)

[9] Xiang Z D, Zeng D, Zhu C Y, Wu D J and Datta P K 2011 *Corros. Sci.* **53** 3426

[10] Kataeva N V, Kositsyn S V and Valiullin 2006 *Mater. Sci. Eng.* A **438–440** 312

[11] Chen D, Chen G L and Ni S 2008 *J. Alloy Comp.* **457** 292

[12] Li C, Hou J and Zhao F G 2012 *Mater. Lett.* **68** 255

[13] Major B 2005 *Sol. Stat. Phen.* **101–102** 181

[14] Chen N X 1990 *Phys. Rev. Lett.* **64** 1193

[15] Zhang W Q, Xie Q, Zhao X D and Chen N X 1998 *Science in China* A **28** 183

[16] Finnis M W and Sinclair J E 1984 *Philos. Mag.* A **50** 45

[17] Zhang S and Chen N X 2002 *Phys. Rev.* B **66** 064106

[18] Long Y, Chen N X and Zhang W Q 2005 *J. Phys.*: *Condens. Matter* **17** 2045

[19] Chen N X, Shen J and Su X P 2001 *J. Phys.*: *Condens. Matter* **13** 2727

[20] Cai J, Hu X Y and Chen N X 2005 *J. Phys. Chem. Sol.* **66** 1256

[21] Qian P, Liu J L, Hu Y W, Bai L J and Shen J 2010 *Chin. Phys.* B **19** 126001

[22] Qian P, Liu J L and Hu Y W 2011 *Chin. Phys.* B **20** 076104

[23] Zhang C H, Han J J, Huang S and Shen J 2011 *Adv. Mater. Res.* **320** 415

[24] Morse P M 1929 *Phys. Rev.* **34** 57

[25] Daw M S and Baskes M I 1983 *Phys. Rev. Lett.* **50** 1285

[26] Daw M S and Baskes M I 1984 *Phys. Rev.* B **29** 6443

[27] Banerjea A and Smith J R 1988 *Phys. Rev.* B **37** 6632

[28] Norskov J K and Lang N D 1980 *Phys. Rev.* B **21** 2131

[29] Rose J H, Smith J R, Guinea F and Ferrante J 1984 *Phys. Rev.* B **29** 2963

[30] Anderson O L 1963 *J. Phys. Chem. Soli.* **24** 909

[31] Zhang B W, Hu W Y and Su X L 2003 *Theory of Embedded Atom Method and Its Application to Materials Science-Atomic Scale Materials Design Theory* (Hunan: Hunan University Press)

[32] Mishin Y, Mehl M J and Papaconstantopoulos D A 2002 *Phys. Rev.* B **65** 224114

[33] Khadikikar P, Locci I, Vedula K and Michal G 1993 *Met. Trans.* A **24** 83

[34] Liu Y P 2004 *Termodynamics Properties and Point Defects of Intermetallics of Al Binary Alloys* (Guangxi: Guangxi University)

[35] Yu S, Wang C Y, Yu T and Cai Jun 2007 *Physica* B **396** 138

[36] Villars P and Calvert L 1997 *Pearson's Handbook Desk Edition*: *Crystallographic Data for Intermetallic Phases* (Materials Park: ASM International)

[37] Hultgren R, Desai P D, Hawkins D T, Gleiser N and Kelly K K 1973 *Selected Values of Thermodynamic Properties of Binary Alloys* (Materials Park: ASM International)

[38] Eskov V M, Samokhval V V and Vecher A A 1974 *Russian Metallurgy* **2** 118

[39] Rzyman K and Moser Z 2004 *Prog. Mater. Sci.* **49** 581

[40] Ren X, Otsuka K and Kogachi M 1999 *Scr. Mater.* **41** 907

[41] Brandes E A 1983 *Smithells Metals Reference Book* (London: Butterworths)

[42] Farkas D, Mutasa B and Ternes K 1995 *Modelling Simul. Mater. Sci. Eng.* **3** 201

[43] Rusovic N and Warlimont H 1977 *Physica Status Solidi* A **44** 609

[44] Wasilewski R J 1966 *Trans. TMS AIME* **236** 455

[45] Dickson R W, Wachtman J B and Copley S M 1969 *J. Appl. Phys.* **40** 2276

[46] Prikhodko S V, Carnes J D, Isaak D G, Yang H and Ardell A J 1999 *Metall. Mater. Trans.* A **30** 2403

[47] Nye J F 1985 *Physical Properties of Crystals* (Oxford: Oxford University)

[48] Beckstein O, Klepeis J E, Hart G L W and Pankratov O 2001 *Phys. Rev.* B **63** 134112

[49] Haines J, Leger J M and Bocquillon G 2001 *Annu. Rev. Mater. Res.* **31** 1

[50] Pugh S F 1954 *The Philosophical Magazine* **45** 823

[51] Gaydosh D J, Jech R W and Titran R H 1985 *J. Mater. Sci. Lett.* **4** 138

[52] Otto J W, Vassiliou J K and Frommeyer G 1997 *J. Mater. Res.* **12** 3106

[53] Goto T, Sasaki T and Hirose Y 1999 *JCPDS—International Centre for Diffraction Data* 518